CHAPTER 1

Introduction and Scope of the Thesis

Contents

CHAPTER 1

Introduction and Scope of the Thesis

1.1 Semiconductor Physics

In last two decades, a significant research interest has been aroused for the novel semiconducting nanostructures to achieve low-cost solution processed photodetectors (Baeg *et al.*, 2013; Jansen-van Vuuren *et al.*, 2016). To fabricate efficient low-cost solution processed photodetectors, material physics of semiconductor plays an important role. In this Ph.D. thesis, solution processed colloidal quantum dots (QDs) of primarily two II-VI semiconductor materials namely the cadmium selenide (CdSe) and zinc oxide (ZnO) have been explored for photo detection applications.

1.1.1 Electronic Structure and Energy Bands

Electronic structure of any material or compound typically depends upon the atom and further the interaction between the multiple atoms or molecules. In a single atom, electrons occupy a certain discrete energy level around the nucleus of the atom (Bohr, 1913; Bohr and Copenhagen, 1913). This original theory was provided by Niels Bohr for the hydrogen atom, and it is commonly referred as Bohr's model shown in Figure 1.1 (a). The electrons can absorb or emit quantized energy to move between the discrete energy levels. The electron will absorb an amount of quantized energy to move from lower energy state to higher energy commonly called *excitation of the electron*. Accordingly, an electron will emit an amount of quantized energy, if electron moves from higher to lower energy level also called *relaxation of the electron*. The quantized

energy absorbed (released) during the excitation (relaxation) of electron is equivalent to the gap between the two energy states. This indicates that the energy states of the atoms are discrete in nature proved by Lyman, Paschen, and Balmer series (Bohr, 1985).

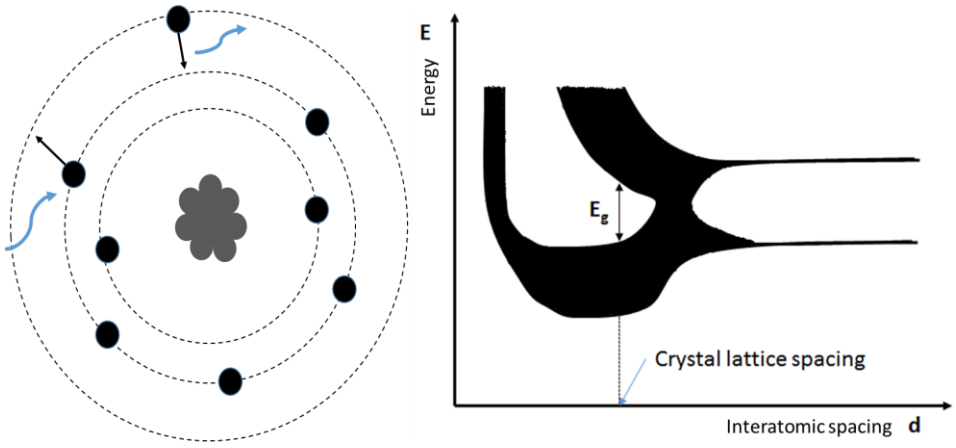

Figure 1.1: (a) Bohr model of the single atom with exciting and relaxing electron and (b) Change in energy bands of the atoms by varying the interatomic spacing.

The energy state of an atom is discrete in nature. In case of a crystal, the discrete energy states of a large number of atoms form the continuous bands of energy states as shown in Figure 1.1 (b). The atoms are arranged in a periodic lattice to form a crystal structure and leads to the interaction or sharing between the electrons present in the outermost shell. This sharing of electrons between the atoms modifies the discrete energy states to continuous energy states. The shaded region shown in Figure 1.1 (b) represents the energy levels allowed for the transition of electrons in the crystal structure (Sze, 2002). The area which lies between the shaded regions is forbidden for electron transition called *forbidden energy gap* and also called a *band gap* of the material. The band which is completely filled with an electron at T = 0 K is called the *valence band*, and another band completely filled with empty energy states (i.e. with no electron) at T = 0 K is called the *conduction band*. When the valence band and

conduction band are overlapped or the band gap energy becomes zero in the case of metals, the energy states in the conduction band are largely filled with free electrons and hence a significant conduction of current becomes very easy by applying an electric field across the metal. The larger the empty energy states in the conduction band of a material, the higher is its resistivity. Such type of materials with empty states in the conduction band are characterized into two categories: *semiconductors* and *insulators*. Semiconductor and insulator can be categorized according to the band gap energy E_g. The insulators have very large band gap with negligible possibility of getting an electron excited from the valence band to conduction band at room temperature. On the other hand, the semiconductors have the moderate band gap energy so that the conduction band can be partially filled with electrons at even room temperature to result in a conductivity in between the insulators and metals. The band gap of energies of CdSe and ZnO, the semiconducting materials from II-VI group, used in this PhD work are 1.74 eV and 3.2 eV respectively. The conductivity of the semiconductors can be controlled by doping and/or by applying some external excitations such as the heat and light depending on the type of applications. For photodetection applications, we are required to apply the light to be detected on the semiconductor to excite electrons from the valence band to conduction band. The photoexcited electrons are finally collected by an electric field to result in a photocurrent proportional to the photon flux density applied on the materials of the photodetectors.

1.1.2 Optical Properties and Excitons

The transition of an electron from lower energy state (valence band) to higher energy state (conduction band) requires an external excitation (energy) which should be equal or more than the band gap of the material. Photodetector works on the

phenomenon of energy transfer from photon to the electron. Photons with sufficient energy can excite electrons from the valence to conduction band of the material.

Table 1.1: Reduced mass μ , static dielectric constant ε_s , exciton binding energy E_B , and Bohr radius a_b of CdSe and ZnO (II-VI group semiconductor material).

Entity	**CdSe**	**ZnO**
Reduced mass μ	0.113 m_o (Meulenberg *et al.*, 2009)	0.109 m_o (Hanada, 2009)
Static dielectric constant ε_s	6.2 (Hui, 2000)	7.40 (Hanada, 2009)
Exciton binding energy	~39.9 meV (Drndić *et al.*, 2002)	60 meV (Özgür *et al.*, 2005)
Bohr radius	5.6 nm (Ekimov *et al.*, 1993)	2.87 nm (Mosquera *et al.*, 2013)

The excited electron occupies an energy state in the conduction band and creates a vacant state in the valence band which is called the *hole*. The excited electron-hole (*e-h*) pairs can be separated by suitable electric field, or they will recombine again leading to *radiative* or *non-radiative* (SRH recombination and Auger recombination) recombination (Larsson, 2011). The electron lying in conduction band and hole in valence band of the electron-hole pairs generated by the incident photons can stay in a bound state called *exciton*. The exciton can be seen as a hydrogen atom with a nucleus (analogous to hole) at center and an electron revolving around it. The energy of a bound state exciton depends upon two factors: one is the interaction energy, also called *binding energy,* E_B, between the electron and hole of the concerned e-h pair; and the

other is the separation length between the electron and hole in the e-h charge pairs, which can be approximated to the *Bohr radius* a_b as a convenient length scale (Klimov, 2010). The binding energy of an exciton and Bohr radius can be described as:

$$E_B = \frac{\mu}{\varepsilon_s^2} R_y \tag{1.1}$$

$$a_b = \frac{\varepsilon_s}{\mu} a_0 \tag{1.2}$$

where R_y is the Rydberg constant and a_0 is the Bohr's radius of the respective values of 13.6 eV and 0.053 nm for the hydrogen atom (Larsson, 2011), μ is the reduced mass and ε_s is the static dielectric constant for the electron-hole pair. The calculated values of $\mu, \varepsilon_s, E_B, a_b$ for the semiconductors CdSe and ZnO of our interest are shown in Table 1.1.

1.2 Quantum Dots

The band gap of the semiconductors is an important parameter to determine its possible applications. For example, silicon (Si) with a band gap of ~1.1 eV at room temperature is suitable for photovoltaic and broadband photodetection applications due to its wide absorption range varying from 400 nm to 1200 nm (Green *et al.*, 2016). On the other hand, external filters may be used in front of Si detectors to achieve a narrowband photodetection by removing the undesired wavelengths of the incident photon density (Lin *et al.*, 2015; Jansen-van Vuuren *et al.*, 2016). However, the band gap of the semiconducting materials can be varied if the size of the semiconducting material is maintained below exciton Bohr radius (mostly below 10 nm) (Klimov, 2010). The generated excitons in such nanocrystals can modify their energy spectrum

according to observed boundaries of the nanoparticles. This phenomenon is known as *quantum confinement effect or quantum size effect* (Klimov, 2010). The quantum size or confinement effect comes into existence when the size of nanoparticles is comparable or less than the natural separation length of the electron-hole pairs. The nanoparticles which follow the aforementioned properties are called quantum dots (QDs).

1.2.1 Structure of Quantum Dots

As mentioned earlier, the physical properties of QDs are highly dependent upon the size of the QDs. These nanocrystal QDs bridges the gap between individual molecules and bulk materials. A single QD can comprise number of atoms ranging from ~100 to ~10000 and accordingly the properties of QDs also lies in between the molecules and bulk materials. More specifically, size, heterostructure, composition, and doping of the QDs define the optical and electronic properties of the QDs. Therefore, QDs can be classified into four different categories:

Binary QDs: Binary QDs consist of an inorganic core overcoated with organic material. The coated organic ligand molecules provide the surface passivation to the dangling bonds present over the surface. The surface passivation offers electronic and chemical stability for the prevention of agglomeration of QDs due to uncontrolled growth. The schematic of binary QDs with surface passivation is shown in Figure 1.2 (a). We observe a significant increase in the surface to volume ratio of a particular volume of material when it is converted into nanoparticles in the form of QDs. In such nanostructured materials, a significant number of atoms of the QDs lies in the surface (e.g., ~ 15 % of the total atoms lies in the surface for a ~5 nm thin CdS QD layer) (Bera *et al.*, 2010).

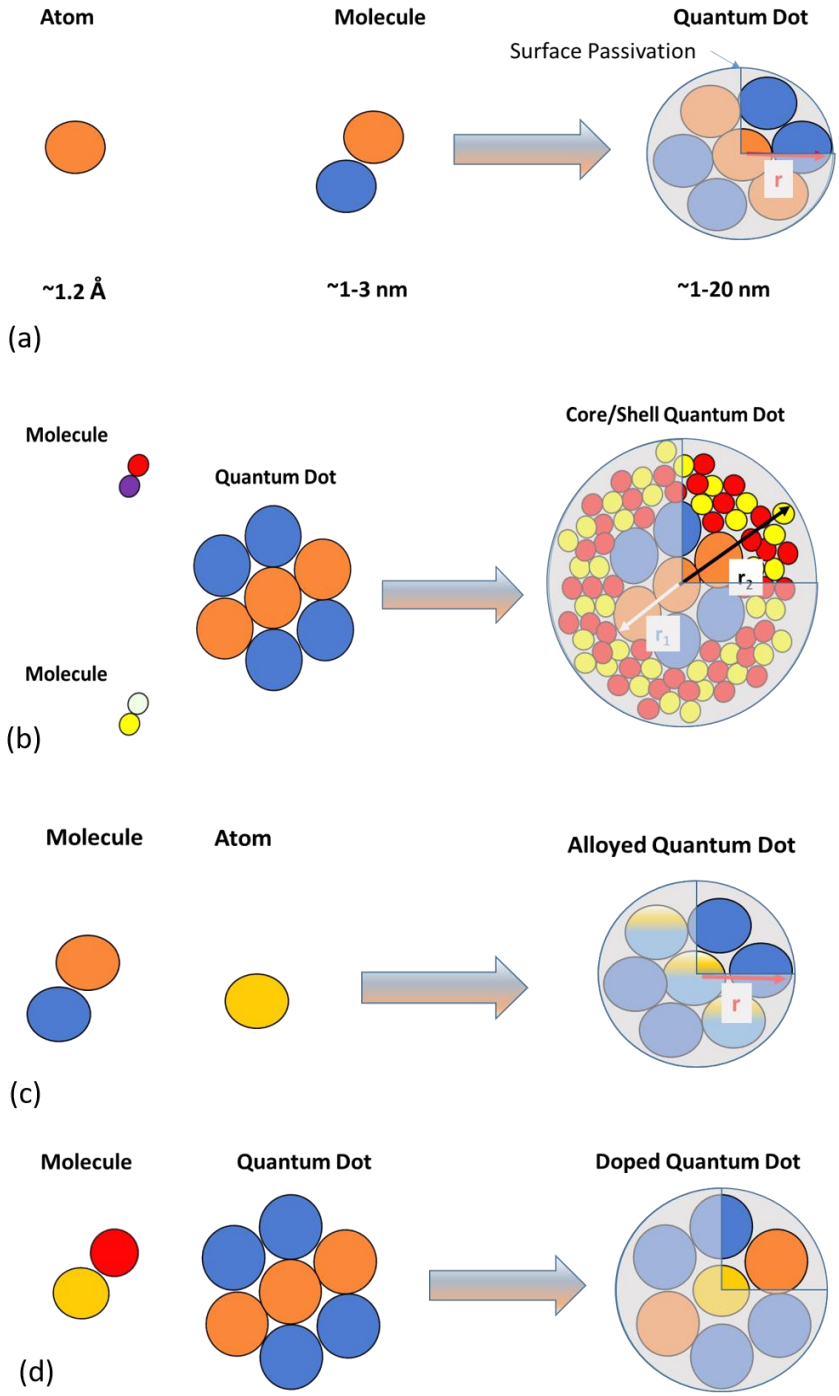

Figure 1.2: (a) Binary QDs, (b) Core-Shell QDs, (c) Alloyed QDs, and (d) Doped QDs.

Because of a large number of surface atoms, the surface defects (or surface trap states) play a significant role in determining the physical properties of such nanostructured materials. These trapping sites restrict the application of such materials

in optoelectronic devices. For example, the sites reduce the transient response time of photodetectors thereby making them unsuitable for high-frequency applications while they reduce the radiative recombination and quenches the quantum yield in light emitting diode applications. Thus it is essential to use a proper surface passivation method to improve the performance of QDs based optoelectronic devices. Different types of surface passivation are used to reduce the trapping sites present in the surface of the QDs to shield the inorganic core from the outer atmosphere to reduce the ageing effect. Thus, the surface passivation is very crucial for optimizing various properties such as the transfer rate of charge carriers, quantum efficiency, luminescent intensity, and stability of the QDs (Bera *et al.*, 2010).

Core-Shell QDs: Core-shell QDs are improved form binary QDs to enhance the properties such as the luminescence, quantum yield and chemical stability of the QDs. The inorganic core with surface defects is over coated by a high bandgap semiconductor such as the zinc sulfide (ZnS) with a band gap of 3.54 eV. The schematic diagram is shown in Figure 1.2 (b). The high band gap materials remove the surface dangling bonds of the core and enhances the confinement of the excitons in all directions. The reduced surface trap states and enhanced excitonic confinements increase the radiative recombination rate, which in turn, improves the luminescence and quantum yield of the material (Murphy, 2002).

Alloyed QDs: Alloyed QDs are achieved by modifying the inorganic material used for the preparation of binary QDs. Such QDs are basically multicomponent QDs used to tune the properties of the QDs by merely changing the composition and internal structure of the QDs without changing their crystallite size. For example, emission of

light of different wavelengths can be achieved in the alloyed semiconductor CdS_xSe_{1-x}/ZnS based QDs of a fixed diameter of ~6 nm by merely changing the composition value *x*. In general, the alloyed semiconductor QDs formed by alloying together two semiconductors of different band gap energies may exhibit interesting properties which are not only different from the properties of their bulk counterparts but also from those of their parent semiconductors. Thus, the alloyed QDs possess novel and additional composition-tuneable properties aside from the properties that emerge due to quantum confinement effects (Shen *et al.*, 2013). The schematic diagram of the alloyed QDs is shown in Figure 1.2 (c).

Doped QDs: QDs passivated with organic molecule ligands provide back to back barrier between the QDs which reduces the charge transfer rate between the self-assembled QDs. Doped QDs are used to improve the electron transfer rate of the QDs by modifying the optical characteristics of the QDs. The schematic diagram is shown in Figure 1.2 (d). The doping in QDs improves the conductivity of the nanostructured material and make them suitable for photovoltaic and photodetection applications (Santra and Kamat, 2012).

1.2.2 Preparation of Quantum Dots

After the first work reported on the preparation of QDs by molecular beam epitaxy (MBE) method in 1970 (Esaki and Tsu, 1970), the research on the fabrication of QDs based devices has been increased exponentially. Some common fabrication methods are discussed in the following.

Stranski-Krastanow Growth: It is one of the popular methods for growing the thin layers of QDs of a material epitaxially at the surface of barrier material. The lattice

mismatch between the material to be deposited and the substrate on which it is to be deposited, the epitaxial layer grown on the substrate will be under strain as shown in Figure 1.3 (a).

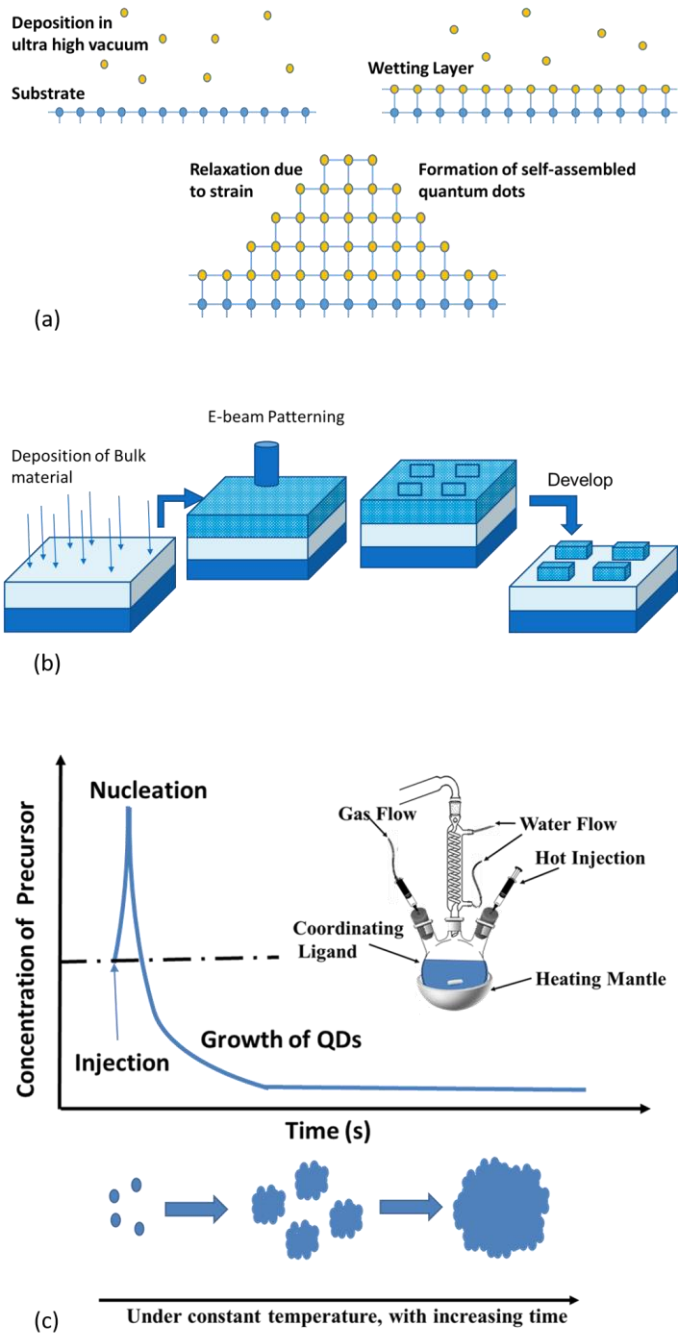

Figure 1.3: (a) Stranski-Krastanow growth mechanism of QDs, (b) Nanoscale patterning method for preparation of QDs, and (c) Schematic of La Mer's model with the experimental setup for preparation of colloidal QDs.

The continuous growth of epitaxial layer will lead to the island-like formation after a certain critical thickness. This island-like formation is due to the reorganization of the energy to achieve stable structure (Drbohlavova *et al.*, 2009; Larsson, 2011). The small island growth structure leads to the formation of QDs in an ordered structure which is called *self-assembly* of the QDs. This process requires highly sophisticated and expensive fabrication techniques to achieve high-order of growth control (in molecular level) such as MBE and metal organic chemical vapor deposition (MOCVD).

Nanoscale Patterning: Patterning techniques used for the preparation of QDs are also called *top-down approach*. It uses a lithography based technology mostly by the combined usage of electron beam lithography and subsequent etching shown in Figure 1.3 (b). The use of lithography techniques to achieve QDs can result in high precision control of QDs positioning. The film of QDs prepared using lithography technique faces several drawbacks such as defect formation, contamination, poor interface quality, and size non-uniformity (Drbohlavova *et al.*, 2009).

Colloidal Nanosynthesis: Since the properties of QDs are size dependent, the achievement of uniformity in the size of the QDs by using low-cost method for QD preparation is highly desirable. Colloidal nano synthesis by *hot injection* method is the most successful route regarding quality, size monodispersity, and preparation cost of QDs (Murray *et al.*, 2001). These QDs are prepared by using the principle of La Mer's growth technique in which hot injection of the precursor is performed on hot coordinating ligands resulting in instant nucleation. The nucleation formation decreases the concentration of precursors and reduces the temperature of coordinating ligand which immediately stops the nucleation process. Further, the reaction follows the

growth of monomers which can be classified into two parts: first is the rapid growth of monomers to form nuclei followed by the stage of slower growth rate called Ostwald ripening or recrystallization (Klimov, 2010). The preparation of QDs starts with quick hot injection followed by nucleation instantaneously for a very short time. This short nucleation time and very long growth time allow achieving monodisperse QDs. Further, the prepared QDs are passivated by an organic ligand which slows the rate of growth of monomers and provides a tool to control the size of the QDs. Schematic of colloidal nano synthesis is shown in Figure 1.3 (c). The prepared QDs are in colloid form and can be easily deposited over any substrate using low-cost solution processed techniques such as spin coating, dip coating, inject-printing (Wood *et al.*, 2009). In this work, we have primarily focused on the QDs prepared by using colloidal nano synthesis technique and spin coating technique for the deposition of the colloidal QDs on the desired substrates.

1.2.3 Electron Transfer in Quantum Dots

The electron transfer between QDs in case of solid thin film is of prominence for the overall efficiency and working of the photodetectors prepared using colloidal QDs. The position of the QDs is fixed and separated by the organic ligand used for surface passivation. The separation and size of QDs define the electron transport properties in a thin film of QDs. The electron transport between QDs can be approximated using Marcus theory (Klimov, 2010):

$$K_{et} = \left(\frac{2\pi}{\hbar}\right)|V_{12}|^2 (4\pi\lambda kT)^{-1/2} \exp(-\Delta E^* / kT) \tag{1.3}$$

where K_{et} is the rate of electron transfer, $|V_{12}|^2$ is the electronic coupling matrix between

initial and final states of transition on resonance. Furthermore, $\Delta E^{*} = \left(\frac{\Delta G^{o} - \lambda}{4\lambda} \right)$ and λ denotes the total reorganization energy for the QDs, where ΔG^{o} is the free energy change between initial and final states shown in Figure 1.4 (a).

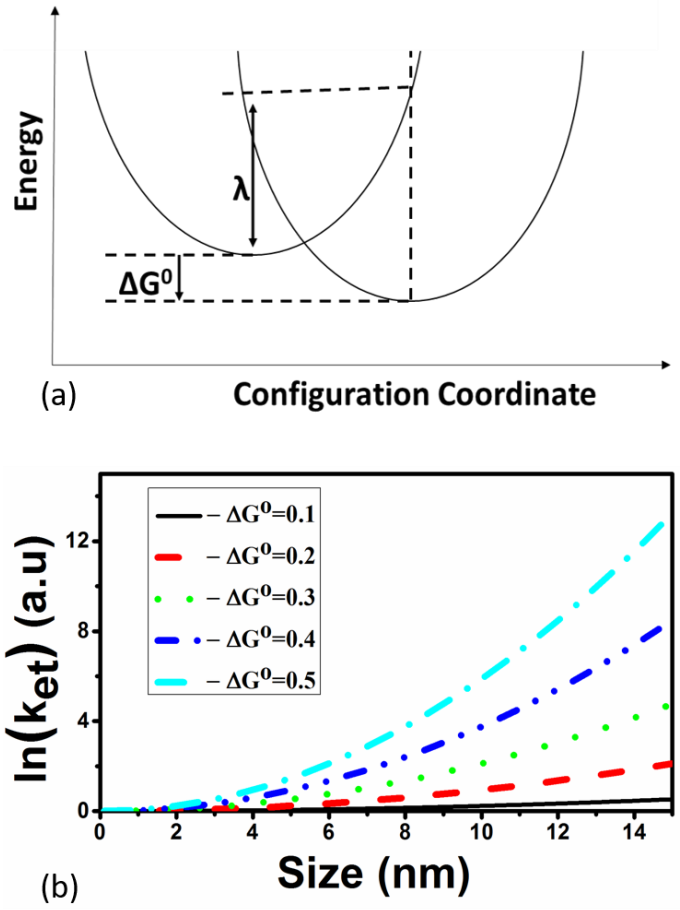

Figure 1.4: (a) Energy as a function of configuration co-ordinate for the initial and final state of the electron transfer (Klimov, 2010), (b) Electron transfer rate for the different values of free energy against the size of the ZnO QDs at room temperature (27 °C) with d = r1 + r2 as the distance between the centers of two QDs with radii r1 and r2 whose boundaries are in contact in the absence of any surface ligands.

Reorganization energy consists of two parts: internal (λ_i) and external (λ_o). The first approximation is done by assuming λ_i to be a constant. The value of λ_o can be approximated by using the following relation (Klimov, 2010):

$$\lambda_0 = \frac{e^2}{4\pi\varepsilon_o}\left(\frac{1}{2r_1}+\frac{1}{2r_2}-\frac{1}{d}\right)\left(\varepsilon_s^*\right)$$

(1.4) where r_1 and r_2 are the radii of two QDs separated by a distance *'d'*. Since the electric field is applied in one direction, Equation 1.3 can be solved by approximating $|V_{12}|^2 \approx S$ where S is the one-dimensional tunneling probability. Thus, $|V_{12}|^2$ can be expressed in terms of the tunnel barrier height (ϕ) and applied field (E) as (Leatherdale et al. 2000):

$$|V_{12}|^2 \approx S = \exp\left(-\frac{4}{3}\sqrt{\frac{2m^*}{\hbar^2}}\frac{1}{eE}\left[\phi^{3/2}-(\phi-eEd)^{3/2}\right]\right) \quad (1.5)$$

Where, The tunneling probability in Equation 1.5 depends upon the size and dielectric constant of the QDs. Further, the thickness of organic ligands providing surface passivation also affect the electron transfer rate between two QDs. Electron transfer rates against the size of the ZnO QD is shown in Figure 1.4 (b). The tunneling probability will decrease exponentially with the increasing barrier width. The other transport phenomenon with the increasing barrier width is hopping of charge carriers from QD to QD. The hopping transport is a field dependent phenomenon, and hopping rate *R(E)* is directly related to the effective mobility of the carriers (Klimov, 2010):

$$R(E) = \frac{\mu_{eff}(E)\times E}{d} \quad (1.6)$$

$$\mu_{eff} = \mu_{free}\frac{n_{free}}{n_{total}} \quad (1.8)$$

where "d" is the hoping distance in the direction of electric field, n_{total} is the total carrier density, n_{free} is the free carrier density, μ_{eff} is the effective carrier mobility, and

hopping rate is the combined effect of $R(E) = R_{forward}(E) - R_{back}(E)$, where $R_{forward}(E)$ and $R_{back}(E)$ are forward and backward hopping, respectively. Since some of the carriers can occupy trap states, effective mobility is smaller than the mobility of the free carriers (n_{free}).

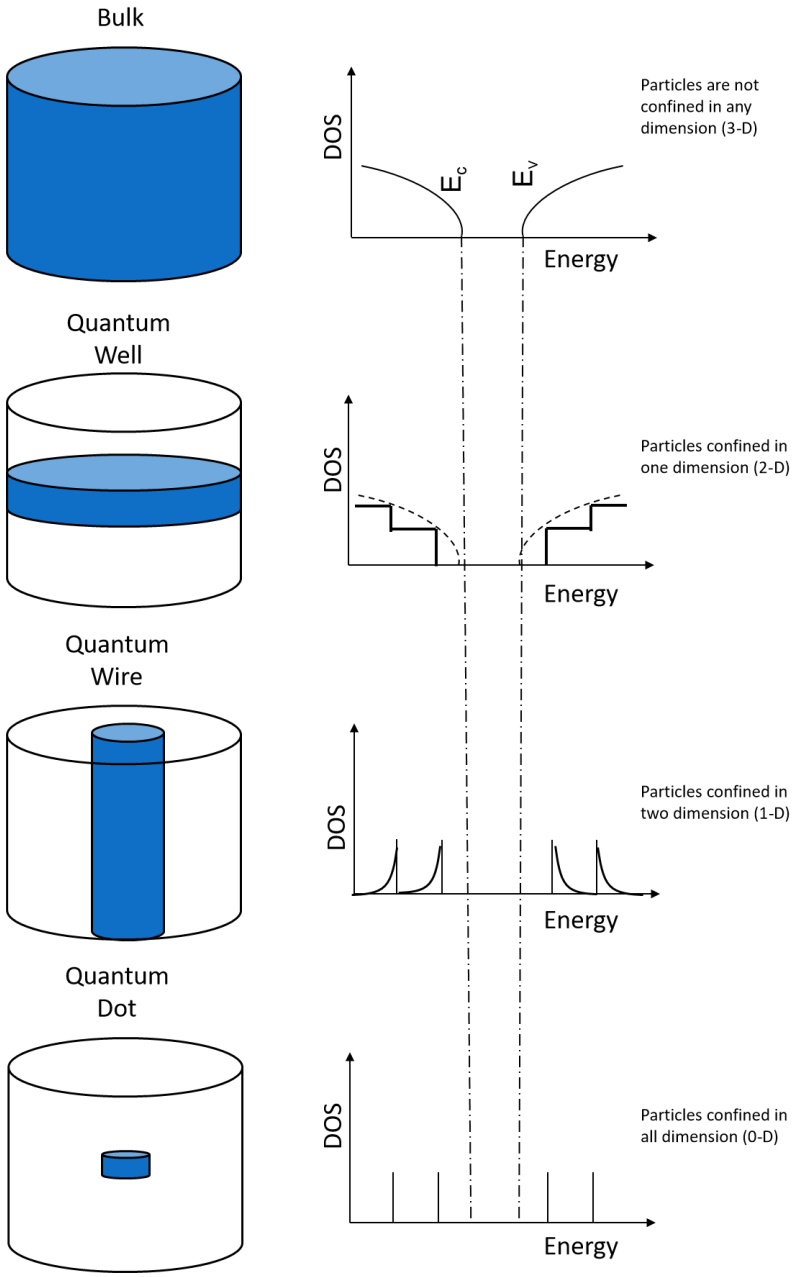

Figure 1.5: Schematic illustration of the changes of the density of states (DOS) with changes in the semiconductor structure from bulk to QDs.

1.2.4 Optical Properties of Quantum Dots

The quantum confinement of the nanoparticle semiconductors varies according to the size of the particles. In the bulk semiconductors, the valence band (E_v) and conduction band (E_c) are continuous due to interactions from other molecules as already discussed in section 1.1.1. As the particles are not confined to the bulk semiconductors, these types of semiconductor structures are called three dimensional (3-D) structure. In the quantum wells, particles are confined only in one dimension due to which the density of states (DOS) is also modified accordingly. The semiconductor structures in which particles are confined in only one direction are called two dimensional (2-D) nanostructures. Similarly, the carrier confinement in quantum wire structures occurs in two directions where the DOS does not remain continuous anymore. These types of nanostructures are called one dimensional (1-D) nanostructures. The particles are confined in every possible direction in the case of QDs. The QDs are called zero-dimensional (0-D) nanostructure. The confinement of particles in QDs leads to the quantization of the conduction and valence band of the nanostructure. The variation of DOS for different types of nanostructures is shown in Figure 1.5. The optical properties of the QDs can be easily assumed as a surface and size-dependent phenomenon (Murray, Kagan and Bawendi, 2000). The quantum confinement of the exciton increases with the decrease in the size of QDs. The band gap (E_g) of the material is also a size-dependent property for the QDs (Klimov, 2010):

$$E_g = \frac{\hbar \alpha_{n,l}^2}{2a^2 m_{eff}^v} + E_{g,0} \tag{1.9}$$

where, $\hbar$ is $h/2\pi$ (with h as the Plank's constant (6.63×10^{-34} m^2kg/s)), $\alpha_{n,l}$ is the n^{th} zero of the Bessel function, a is the radius of the QDs, m_{eff}^v is the effective mass of the

free particle, and $E_{g,0}$ is the energy of state at *k* (wavenumber) = 0. From Equation 1.9, it can be easily deduced that $Eg \propto 1/a^2$. Thus the band gap of the QDs shows a blue shift with the decrease in the QDs size. The quantization of energy states and shifting in the band gap of QDs can be utilized to achieve tuneable spectrum selective photodetectors.

1.3 Colloidal CdSe and ZnO Quantum Dots Characterization Techniques

Characterization of nanostructured materials provides the information regarding their possible electronics and optoelectronic applications. In this section, a brief discussion about various characterization techniques and their basic principles of operation are presented.

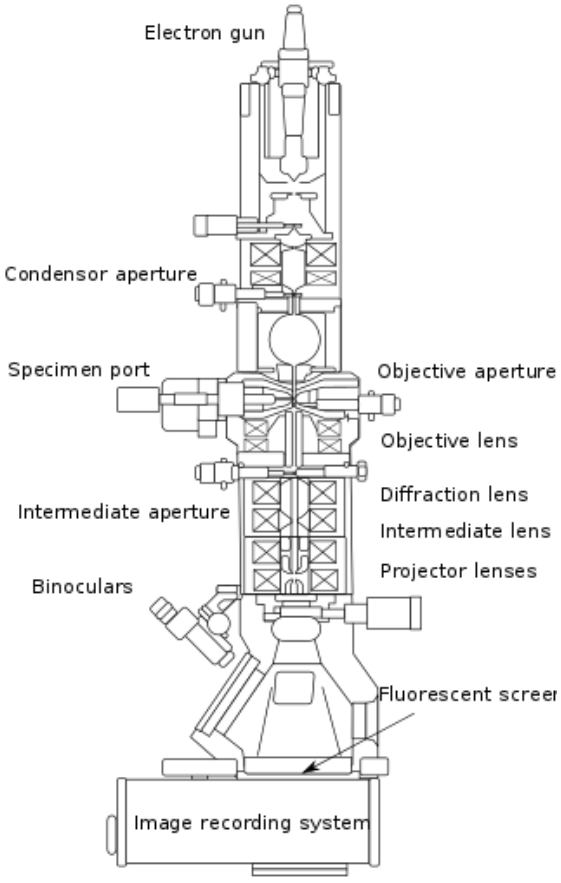

Figure 1.6: Schematic diagram of Transmission Electron Microscopy (TEM) (By Gringer (talk) - Commons: Scheme TEM, CC BY-SA 3.0, https://commons.wikimedia.org/w/index.php?curid=5624170).

1.3.1 Structural Characterization

The structural properties of the nanomaterials play a vital role in determining their applications. The commonly used structural characterization techniques are described briefly in the following.

Transmission Electron Microscopy (TEM): Transmission electron microscopy (TEM) is a microscopy technique based on the electron transmittance phenomenon through the sample. The schematic of the TEM measurement setup is shown in Figure 1.6. The transmitted electrons intensity varies according to the sample and these variations in the electrons intensity and contrast form an image of the sample. The TEM is used to provide the imaging of the surface at a very high resolution due to the smaller de Broglie wavelength of electrons (Voutou, Stefanaki and Giannakopoulos, 2008). This enables the instrument to capture fine details such as a single column of atoms which is thousands of times smaller than a resolvable object seen in an optical microscope.

Selected Area Electron Diffraction Pattern (SAED): Selected area electron diffraction pattern (SAED) is used for crystallographic measurements using TEM. In the case of SAED measurements, the wave nature of the electrons is assumed instead of particle nature due to the wavelength of high energy electrons in few thousandths of a nanometer (Voutou, Stefanaki and Giannakopoulos, 2008). The inter-atomic spacing in solids is about a hundred times larger than the wavelength of the incident electrons. Thus, the atoms diffract the incident beam of electrons, and some portions of the incident electrons are scattered to particular angles proportional to the crystal structure of the sample. These scattered electron beams provide the information regarding the

structural properties such as the lattice, crystal orientation and crystalline nature of the crystals.

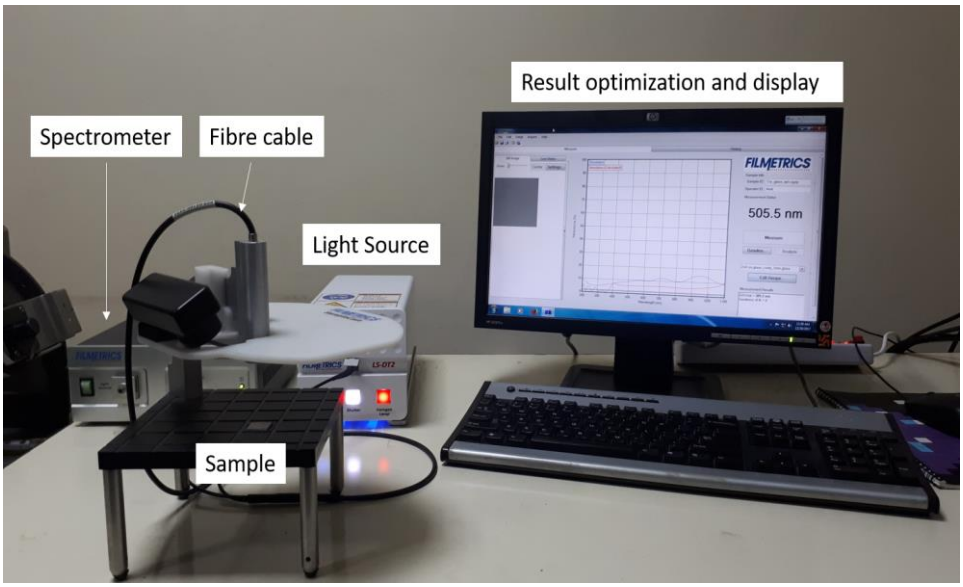

Figure 1.7: Experimental measurement setup for spectrophotometry.

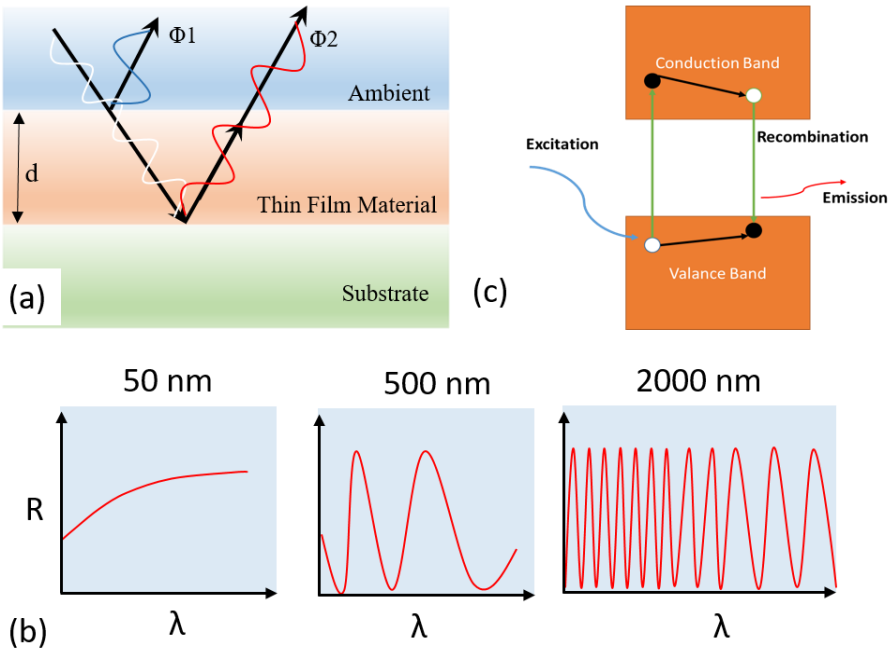

Figure 1.8: (a) Interaction of incident light wave with the thin-film material at the incoming and outgoing interface, (b) Variation in the oscillations of the light wave due to the thickness of the thin-film, and (c) Photoluminescence due to excitation and recombination of an electron-hole pair.

1.3.2 Optical Characterization

The optical property of a material depends upon the structural, morphological, and electronic properties. Thus, the optical characterization techniques provide information regarding the possible application of the material in optoelectronic devices.

***Spectrophotometry*:** The measurement setup used for spectrophotometry is F−20 UV Analyzer, Filmetrics is shown in Figure 1.7. It is used to measure the reflectance and transmittance of characteristics of the nanostructured thin films. The above results can be easily used to calculate the absorption and band gap characteristics of the thin films. The thickness of the thin film is calculated by measuring the oscillations produced by light when encountering with the interfaces as shown in Figure 1.8 (a) & (b). The oscillations are optimized using DFT (Discrete Fourier transform) and FFT (Fast Fourier Transform) algorithms along with the material characteristics such as the *n* (refractive index) and *k* (extinction coefficient). A good match between the theoretical and experimental results measured via spectrometer verifies the accuracy of the result for the thickness of the film.

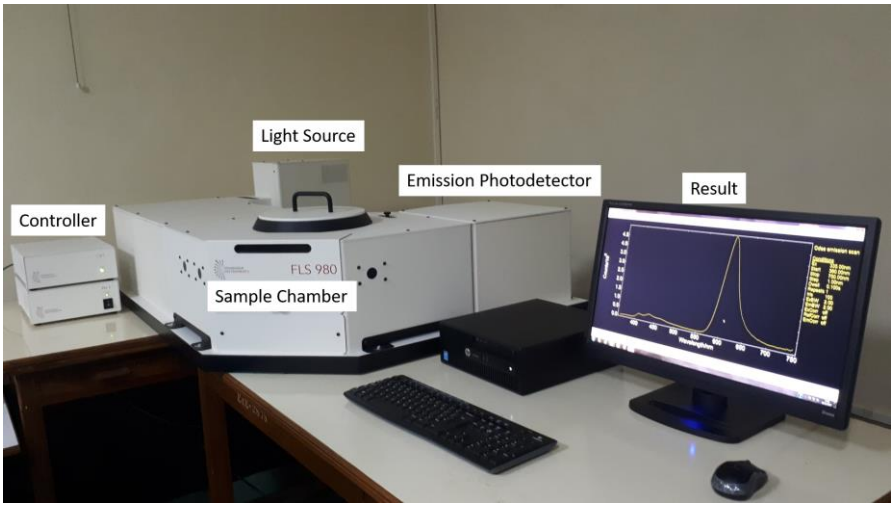

Figure 1.9: Experimental measurement setup for photoluminescence spectrometry.

***Photoluminescence Spectrometry*:** Photoluminescence (PL) spectrometry is another non-destructive measurement technique used for the materials in various forms: thin film, powder form, and solution. The PL is the emission of light from nanomaterial or any other form of matter after the absorption of photons shown in Figure 1.8 (c) (Murphy, 2002). The emission of light depends upon various factors such as band gap of the material and defects or surface traps (Murphy, 2002). The PL results can be used to extract the vital information regarding the band gap of the QDs since it is directly associated with the particle size of the QDs. The PL of QDs are largely affected by the surface and can be treated as a surface effect due to the high surface to volume ratio of QDs (Klimov, 2010). The experimental setup used for PL measurement using FLS 980 from Edinburg Photonics is shown in Figure 1.9.

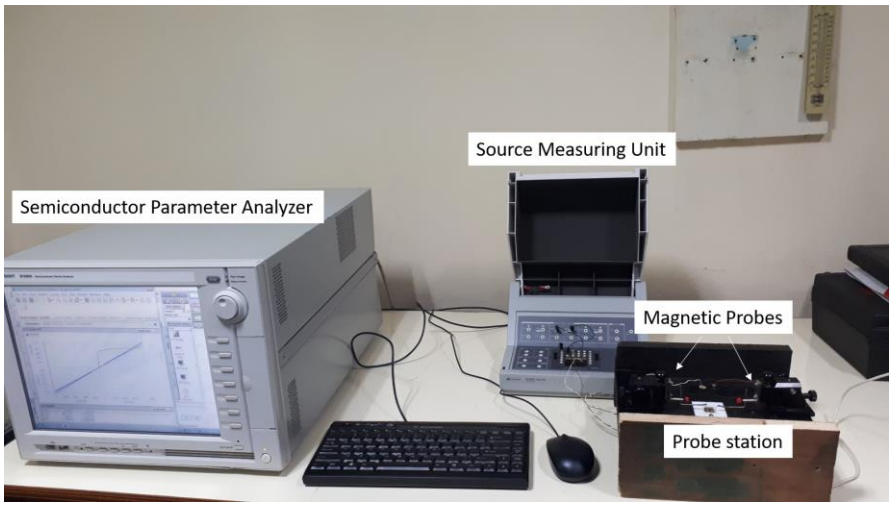

Figure 1.10: Experimental measurement setup for electrical characterization.

1.3.3 Electrical Characterization

In this section, we will discuss the techniques used to determine the electrical parameters of the photodetectors fabricated using colloidal QDs of ZnO and CdSe. Electrical characterization can be used to determine various properties such as the

barrier height, ideality factor, carrier concentration, and depletion width of any metallurgical p-n junction. The current-voltage and capacitance-voltage characteristics of the devices are studied by using Keysight B1500A as shown in Figure 1.10.

Current-Voltage measurement: Current-Voltage (*I-V*) characteristics provide the relationship between the current flowing through an electronic device and the voltage across applied its terminals. In this work, we have mainly characterized photodiodes to determine their barrier height and ideality factor.

Capacitance-Voltage measurement: Capacitance-Voltage (*C-V*) characteristics provide the variation in the junction capacitance in a diode with to the change in the sweeping voltage applied across the terminal of the device. The *C-V* characteristics of any diode depend on its junction properties. The measured C-V characteristics can be used to extract the carrier concentration, depletion width, and barrier height of any junction with known doping profile.

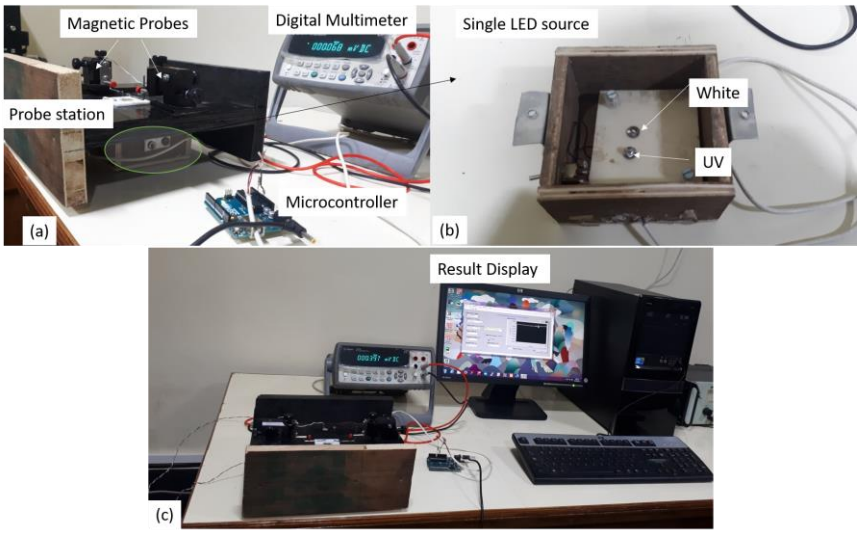

Figure 1.11: (a) Experimental measurement setup for time response measurement, (b) Single LED (UV and White) source for device excitation, (c) Complete time response measurement setup with data acquisition using LabView.

1.3.4 Photoresponse Characterization

Photoresponse characteristics are very important for the performance characterization of the photodetector devices in which the I-V characteristics can be modified by an incident beam of photons with energy greater than the band gap energy of the active material of the device.

***Temporal or Time Response Measurement*:** The response time is an important performance parameter of the photodetectors. The response time of the photodetector is determined by the lifetime "τ" of the charge carriers. The required time to change the current from 10% to 90% of the maximum value upon the illumination of the light is called *rise-time*. In a similar manner, the change in current from 90% to 10% of the maximum value when the light is turned off is called *fall-time*. The small values of the photodetectors make them suitable for high-speed applications. The complete in-house prepared time response measurement setup is shown in Figure 1.11.

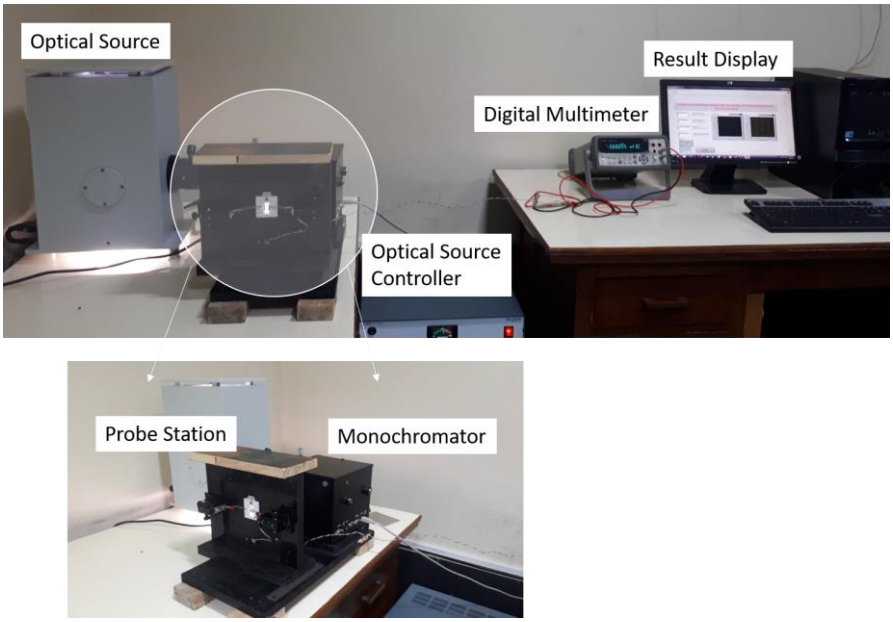

Figure 1.12: Experimental measurement setup for photocurrent measurement (automated data acquisition is achieved using LabView).

Photocurrent-Wavelength Measurements: The operational wavelength of the photodetector defines the application of photodetector in the Ultra-Violet (UV), Visible, or Infrared region (IR) region. The variation of photocurrent over the complete wavelength spectrum is thus important for characterizing photodetectors. The monochromatic wavelength is used as an exciting source for the photodetector. The wavelength is varied over a specified range, and the photocurrent is recorded for every incident wavelength. The complete in-house prepared measurement setup for photocurrent versus wavelength characteristics using LabView is shown in Figure 1.12.

1.4 Some State-of-the-art Works on Colloidal QDs Based Photodetectors

The objective of the present thesis is to fabricate and characterize some solution-processed ZnO and CdSe QDs based photodetectors. The CdSe and ZnO are direct bandgap II-VI group semiconducting materials with band gap energies of 1.74 eV (Jin *et al.*, 2012) and 3.37 eV (Liu, Sakurai and Aono, 2010), respectively. The QDs of these materials show a blue shift with the decrease in their size as discussed earlier. In general, the CdSe QDs show the optical absorption in the visible region while the ZnO QDs show the absorption over the ultra-violet (UV) region. We will now review some important literature on the use of colloidal CdSe and ZnO QDs for photodetection applications.

1.4.1 Review of Self-Powered Photodetectors

The photodetectors have wide applications in the field of cameras, non-destructive testing, mimicking artificial eye, and computing systems (Jansen-van Vuuren *et al.*, 2016). The traditional photodiodes usually require an external supply to operate the device under reverse bias conditions (Rawat *et al.*, 2016). On the other hand, the self-

powered photodiodes may not require any external power supply and mostly work under either photovoltaic short-circuit or open-circuit mode (Bera *et al.*, 2016). Inorganic-based self-powered photodetectors are lucrative since they usually provide a high absorption coefficient for the incident light and high mobility of carriers (Bera *et al.*, 2016). However, the major drawback of inorganic material based self-powered photodetectors is the requirement of high-temperature fabrication process (Jin *et al.*, 2012; Gao *et al.*, 2013). Gao et al. (Gao *et al.*, 2013) and Jin et al. (Jin *et al.*, 2012) have reported a very high responsivity (>8 A/W) in CdSe nanobelts (NBs) based self-powered photodetectors fabricated at a high-temperature (~1000ºC). Note that high-temperature fabrication processing consumes a lot of power and hence defeats the purpose of self-powered photodetectors. Some works also show the requirement of high-temperature fabrication of self-powered photodetectors (Oertel *et al.*, 2005; Xie *et al.*, 2013; Game *et al.*, 2014; Nusir *et al.*, 2014; Bera *et al.*, 2016). Researchers have also used hybrid self-powered photodetector structures fabricated at low temperatures (Xie *et al.*, 2013; Game *et al.*, 2014; Bera *et al.*, 2016). The hybrid photodetectors use the combination of organic and inorganic semiconductors to achieve the benefits of high carrier mobility and high absorption coefficient of inorganic materials and the low-temperature fabrication processing property of organic materials simultaneously (Oertel *et al.*, 2005; Xie *et al.*, 2013; Game *et al.*, 2014; Bera *et al.*, 2016; Yu, Zhang, Song, *et al.*, 2017; Yu, Zhang, Zhang, *et al.*, 2017; Zhang *et al.*, 2017). Xie et al. ((Xie *et al.*, 2013)) have reported a self-powered photodetector using TiO_2 nanorods as the inorganic material and spiro-MeOTAD as the organic material. The spiro-MeOTAD organic thin film is used as the active absorbing layer while the TiO_2 is used as Electron transport layer (ETL). They (Xie *et al.*, 2013) have prepared inorganic TiO_2 thin film at ~500°C

and achieved a maximum photoresponsivity of 0.01A/W at 410 nm at 0 V bias. Game et al. (Game *et al.*, 2014) have used n-ZnO nanorods with organic spiro-MeOTAD thin film for fabricating a self-powered photodetector. They (Game *et al.*, 2014) have prepared nitrogen-doped ZnO nanorods at ~450°C to achieve a 6 mA/W at 470 nm. Bera et al. (Bera *et al.*, 2016) have prepared a hybrid self-powered photodetector using Sb_2S_3 with spiro-MeOTAD. They (Bera *et al.*, 2016) have processed Sb_2S_3 at ~450°C to achieve a responsivity of 8.7 mA/W at 475 nm with a rise time and fall time of 25 ms. Oertel et al. (Oertel *et al.*, 2005) have reported a low-temperature (70°C) processed ITO/PEDOT: PSS/CdSe QDs/Ag photodetector using CdSe QDs as the active layer in the device. They (Oertel *et al.*, 2005) have obtained a very poor response with the external quantum efficiency (EQE) of 0.12% at 540 nm and 0.23% at 350 nm under an applied bias of 0 V.

1.4.2 Review of Spectrum Selective Photodetectors

Spectrum selective photodetectors with high detectivity, high signal-to-noise ratio, and fast response speed are important devices for multiple applications such as digital cameras, optical communication, flame sensing, and water sterilization (Monroy, Calle and Beaumont, 2001; Aufiero *et al.*, 2006). Spectrum selectivity of the photodetectors defines the ability to detect accurate and intended energy photons. Jansen Van Vuuren et al. (Jansen Van Vuuren *et al.*, 2010) have theoretically defined the limit of Full width at half maximum (FWHM) (<100 nm) for independent detection of the photons of different energies. Researchers have reported various spectrum selective UV (Qin *et al.*, 2013; Kumar *et al.*, 2017), Visible (Um *et al.*, 2011; Lin *et al.*, 2015) and NIR/IR (Qiao *et al.*, 2016) based photodetectors using an additional filter layer (Qin *et al.*, 2013; Qiao *et al.*, 2016) or using active layer engineering (Um *et al.*, 2011; Lin *et al.*, 2015; Kumar

et al., 2017). Qin et al. (Qin *et al.*, 2013) have reported a wavelength selective p-GaN/ZnO photodiode by using additional composites as a filter layer from the back side. They (Qin *et al.*, 2013) have achieved a peak responsivity < 0.15 mA/W at 350 nm while illuminating the device from the back side. Lin et al. (Lin *et al.*, 2015) have reported filter-less spectrum selective photodetectors for the visible region using perovskites treated with different types of dyes. They (Lin *et al.*, 2015) have fabricated blue, green, and red photodetectors with an FWHM < 100 nm. The colloidal QDs are also used to achieve a spectrum selective photodetectors by tuning the absorption of the particles by varying the particle size of QDs (Kumar *et al.*, 2017). Qiao et al. (Qiao *et al.*, 2016) have reported a narrowband photodetector with an FWHM of ~100 nm and a responsivity < 1 A/W at a very high voltage of 10 V. In their work, they (Qiao *et al.*, 2016) have used PbS QDs as an active layer and perovskite layer as a filter for short wavelength photons.

1.4.3 Review of Other Colloidal QDs Based Photodetectors

Colloidal QDs are widely used in the solution processed techniques (Pal *et al.*, 2012) for low-cost, large-area fabrication and convenient material integration of thin film photodetector (PD) devices. Singh el al. (Singh *et al.*, 2007) have reported polarization-sensitive photodetectors using solution-synthesized CdSe nanowire (NW) prepared at 330°C. They (Singh *et al.*, 2007) achieved a responsivity of ~0.17 A/W at an applied bias of 35 V under the illumination power of 100 nW. Pourret el al. (Pourret, Guyot-Sionnest and Elam, 2009) fabricated photodetectors using CdSe QDs for active layer and ZnO deposited by atomic layer deposition for acting as the ETL. They (Pourret, Guyot-Sionnest and Elam, 2009) have achieved a responsivity of 5.7×10^{-6} A/W at an applied bias of 1 V under the illumination at 532 nm. Coates et al. (Coates *et*

al., 2010) have fabricated CdSe QDs based photoconductor on which QD synthesis and sintering occur simultaneously on the substrate at 450°C. They (Coates *et al.*, 2010) have reported a responsivity of 12 A/W at an applied bias of 12 V at an illumination wavelength of 720 nm. Hegg et al. (Hegg *et al.*, 2010) have fabricated a CdSe/ZnS QDs based photoconductor with a nanogap of 250 nm. After annealing at ~300°C, they (Hegg *et al.*, 2010) have obtained a responsivity of 5.88×10^{-3} A/W at the illumination wavelength of 405 nm of optical density 17 pW/cm^2. Xing et al. (Xing *et al.*, 2012) have fabricated a photoconductor with CdSe nanocrystals deposited using electrodeposition within a gold nanogap (>50 nm) prepared by feedback-controlled electromigration. In their work, they (Xing *et al.*, 2012) have achieved a responsivity of 31 A/W at an applied bias of 1 V under the illumination wavelength of 532 nm of 0.9 W/cm^2 optical power density. Similarly, Nusir et al. (Nusir *et al.*, 2014) have fabricated a low-temperature CdSe nanocrystal-based metal-semiconductor-metal (MSM) photodetector with an interdigitated separation of 5 μm and found the detectivity of 3.5×10^{10} Jones at an applied bias of 5 V. Adinolfi et al. (Adinolfi *et al.*, 2015) have reported a PbS QDs based photo-JFET with a MoO_3 layer on it to deplete the active channel (PbS QDs) of the photo-JFET and the incident light to act as the gate control. Pal et al. (Pal *et al.*, 2012) have reported a p-n junction photodiode using PbS QDs as an active layer. In their work, they (Pal *et al.*, 2012) have reduced the dark current without reducing the external quantum efficiency (~80%) and achieved a very high detectivity of 10^{12} Jones.

1.4.4 Other Application of Colloidal CdSe and ZnO Quantum Dots

***Photovoltaic Devices*:** The QDs are the emerging nanomaterials with the large surface-to-volume ratio which can be easily explored for the fabrication of large-area

low-cost solar cells (Chuang *et al.*, 2014). The band gap tuning property of the QDs by just changing the particle size can be explored for multiple spectrum selective photodetectors. The QDs can be used to achieve the absorption region similar to that of the solar spectrum by simply stacking of multiple sized QDs of single or multiple compound materials in the form of thin films (Wang *et al.*, 2011). ZnO QDs are widely used as an ETL in solar cell fabrication (Ko *et al.*, 2016), and CdSe QDs sensitized solar cells for improvement of efficiency (Salant *et al.*, 2010).

***Bio-Sensing*:** QDs are widely used in the field of pH sensing with ion probes, luminescence sensors (Deng *et al.*, 2007; Suzuki *et al.*, 2008; Tang, Lee and Achilefu, 2012). CdSe QDs based thin film devices show the repeatable and stable response for pH sensing (Kumar *et al.*, 2014). Quantum yield of the QDs based device can be tuned easily by changing the precursor concentration or the size of the QDs, which can be used for cancer detection (Liu *et al.*, 2007)

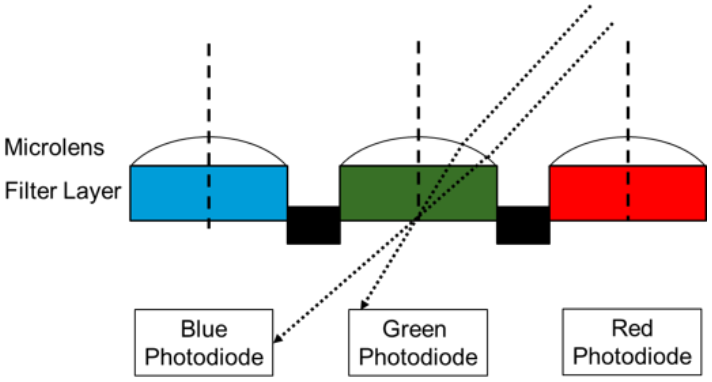

Figure 1.13: Implementation of spectrum selective photodetectors using filter layer and cross-talk between the detectors.

1.4.5 Major Observation from the Literature Survey

Colloidal QDs are the emerging nanomaterials with the large surface-to-volume ratio which can easily be used to fabricate self-powered, spectrum selective, and low-

cost photodetectors. To achieve self-powered photodetectors, colloidal CdSe QDs provide the competitive option against the other inorganic materials regarding the low-temperature synthesis. The preparation and synthesis of colloidal QDs based photodiodes are low-power consuming (w.r.t fabrication and processing temperature) as the solution of the QDs can be processed without any crystallization temperature (Oertel *et al.*, 2005). With current technology, Si photodetectors used in combination with Bayer's filter (Bayer, 1976) to achieve the spectrum selective photodetection. Thus the Si-based spectrum selective photodetectors not only increases the complexity and fabrication cost of the detectors but also reduces the overall quantum efficiency of the detection system (Guttosch, 2005). The involvement of external Bayer's filter also leads to the crosstalk between the spectrum selective photodetectors (Guttosch, 2005) as shown in Figure 1.13. The application of colloidal QDs in photodetectors can be used for high-speed imaging and communication applications due to their very low noise with very fast response time.

1.5 Motivation and Problem Definition

The use of colloidal QDs for photodetection applications requires extensive study regarding device engineering and material engineering. Dark current or noise current plays an important role in determining the overall performance of the photodetectors. To reduce the dark current, researchers use multiple approaches including variation in the semiconductor-metal interface (Agostinelli *et al.*, 2008) and device structures (Ng *et al.*, 2008; Ramuz *et al.*, 2008). The implementation of CdSe QDs as an active layer (absorbing layer) requires a charge transport layer of wide bandgap material to extract photo-generated charge carriers efficiently. Among various metal-oxides explored for

the charge transport layers in the photodetectors, colloidal ZnO QDs are the most promising material for ETL (Chen *et al.*, 2014) due to its strong radiation hardness, high chemical stability, low-cost, large band gap (~3.3 eV) and high exciton energy (60 meV) (Liu, Sakurai and Aono, 2010). However, since the size of the QDs defines the electrical transport properties (Drndić *et al.*, 2002) of the photodetectors, optimized electron transport layer will enhance the photoresponse and reduce the noise current simultaneously. Effect of the heat treatment is a widely used technique for enhancing the device stability and photoresponse (Yadav, Pandey and Jit, 2014). The annealing of charge transport layers can be used to optimize charge trapping states and roughness of the thin film to define the performance of the photodetectors (Yu *et al.*, 2013). Further, an analysis of ETL (ZnO QDs)/HTL (MoO_x) is required to optimize the device efficiency parameters.

The fabrication of conventional self-powered inorganic or hybrid photodetectors reported in the literature require high-temperature processing. High-temperature processing consumes a lot of power and defeats the purpose of self-powered photodetectors. The colloidal CdSe QDs can be used to achieve low-temperature processed self-powered photodetectors with ZnO QDs as an ETL. Further, the integration of CdSe QDs with organic material such as the poly (3, 3’’’-dialkylquaterthiophene) (PQT-12) can help in additional reduction in operating temperature. The operation of self-powered photodetectors can also be made spectrum selective. The traditional spectrum selective photodetectors trade off with their figure of merit (responsivity) to achieve spectrum selectivity (narrow FWHM). The sandwiched CdSe QDs between the two high work function materials (ZnO QDs and Pd) can be

used to achieve spectrum selectivity with the increased figure of merit by optical resonance.

1.6 Scopes of the Thesis

We have already discussed that colloidal QDs are novel materials with the versatile properties which can be easily tuned and modified by varying the size and material of the QDs. The self-powered photodetectors can work without an external power source which can be explored for the next-generation optoelectronic devices to operate wirelessly and independently. On the other hand, the spectral selectivity of the photodetectors enables the detectors to detect a particular wavelength of light which can be used for futuristic applications such as artificial vision, image scanners, and image sensors. Given the above observations, the present thesis has been designed to report the fabrication and characterization of some CdSe, and ZnO colloidal QDs based low-cost, self-powered and spectrum selective photodetectors using solution processed methods. The thesis consists of SEVEN chapters including the present chapter. The outline of the remaining chapters is given below.

Chapter 2 presents the effect of heat treatment of the colloidal ZnO QDs based ETL on the performance of ZnO QDs/CdSe QDs/ MoO_x based photodetectors where the colloidal CdSe QDs layer acts as an active layer and the thermally deposited MoO_x thin film layer acts as a hole transport layer and the colloidal ZnO QD acts as the ETL. The effect of annealing at 250, 350 and 450°C of the ZnO QDs thin film (i.e., ETL) on the device performance is annealed. The optimum annealing temperature of the ZnO QDs ETL has been investigated for achieving the minimum dark (noise) current and maximum photoresponse of the detector. The ZnO QDs thin films annealed at the

optimized temperature has also been applied in the thin film transistors to improve their performance.

Chapter 3 discusses the effect of heat treatment on the performance of ZnO QDs/MoO_x heterojunction based photodetectors. The colloidal ZnO QDs have been first deposited on the ITO coated glass substrates. Two types of heterojunction devices are fabricated. In the first type of device, the MoO_x is deposited on the ZnO QDs layer by sol-gel method while the MoO_x layer is grown on the ZnO QDs layer by thermal deposition in the second type of device. Thermally deposited Ag film (~50 nm) is grown on both the solution processed and thermally deposited MoO_x films using shadow mask technique to act as the anode whereas the ITO acts as a cathode in the device. Both types of heterojunctions are annealed after device fabrication to analyze the effect of heat treatment on the electrical and optical properties of the ZnO QDs/MoO_x heterojunction based photodetectors under study in the present chapter.

Chapter 4 presents the fabrication and characterization of colloidal CdSe and ZnO QDs based inorganic self-powered photodetectors. In this work, we have used n-Si/ZnO QDs/CdSe QDs/Au structure where the ZnO QDs thin film is used as the ETL whereas the colloidal CdSe QDs thin film is used as the active layer in the device. The optical and electrical properties of the device are discussed in details. Finally, the photoresponse properties such as the transient response, responsivity, and detectivity measured at 0 V of the self-powered photodetector have been discussed.

Chapter 5 reports the fabrication and characterization of colloidal CdSe QDs and PQT-12 based self-powered hybrid photodetector. In this work, we have used an ITO-coated-glass/PQT-12/CdSe QDs/Au structure where the CdSe QDs layer is used as the

active layer, and the PQT-12 layer is used as the charge transport cum filter layer. The photoresponse characteristics of the hybrid self-powered photodetector are analyzed using the optical properties of PQT-12 and CdSe QD thin films.

Chapter 6 presents the fabrication and characterization of a colloidal CdSe and ZnO QD based spectrum selective photodetector. In this work, the device structure consists of the active layer of CdSe QDs sandwiched between a colloidal ZnO QDs layer and a metal electrode (of Au or Pd). The measurements for the transient response, responsivity, detectivity and external quantum efficiency (EQE) of the proposed structures at 0 V bias voltage are discussed. The effects of Au and Pd metal electrodes on the full width at half maximum (FWHM) of the photoresponse characteristics of the photodetector have been analyzed.

Finally, ***Chapter 7*** of the thesis has been designed to include the overall summary and conclusion of the work discussed in the present thesis. This chapter also provides some future scope of the works related to the present area of research.